Medina and Sampaio-Neto *EURASIP Journal on Wireless Communications and Networking* 2011, **2011**:80
http://jwcn.eurasipjournals.com/content/2011/1/80

EURASIP Journal on
Wireless Communications and Networking
a SpringerOpen Journal

RESEARCH Open Access

Frequency domain equalization space-time block-coded CDMA transmission system

César Augusto Medina* and Raimundo Sampaio-Neto

Abstract

In this work we propose a space-time block-coded (STBF) CDMA transmission system suitable for use with frequency domain equalization (FDE) algorithms. We illustrate the FDE by implementing the maximal ratio combining, the zero forcing and the minimum mean squared error single user detection algorithms. A diversity gain analysis is developed and some interesting results are pointed out. It is shown through computer simulations that the proposed transmission system exhibits good performance in terms of bit error rate when compared to previously proposed STBC CDMA transmission systems.

Keywords: frequency domain equalization (FDE), space-time block-codes (STBC), single carrier CDMA transmission systems, multicarrier CDMA transmission systems

1 Introduction

Space-time block-codes (STBC) schemes have emerged as a powerful transmit diversity technique to combat fading in wireless communications. One of the most successful space-time coding scheme was first proposed by Alamouti [1] for the case of two transmit and multiple receive antennas. Further developments for more than two transmit antennas were later reported on [2,3], and it was shown that the Alamouti's scheme is the only existing complex orthogonal design, with full rate, full diversity and minimal delay. STBC was applied for direct-sequence code division multiple access (DS-CDMA) transmission system in [4,5]. All the aforementioned systems [1,5], assume flat-fading channels and suffer performance degradation in frequency-selective channels. Some STBC schemes to deal with frequency selectivity have been proposed for orthogonal frequency division multiplexing (OFDM) [6], single-carrier (SC) time-domain equalization [7] and single-carrier frequency-domain equalization (SC-FDE) systems [8,9].

The complexity and performance of SC-FDE systems are comparable to that of OFDM systems while avoiding drawbacks associated with multicarrier (MC) implementation. On the other hand, SC systems cannot certainly offer the same flexibility as OFDM in the management of bandwidth and energy resources [10] and FDE does not represent an optimal solution to signal detection over frequency-selective channels due to intersymbol interference (ISI). In [11], adaptive algorithms to mitigate ISI effects for frequency domain equalization (FDE) in frequency-selective channels were proposed.

STBC CDMA-based transceivers for frequency-selective channels have been studied in [12-16], using a structure similar to the one proposed in [4,5] for the case of flat-fading channels. A different structure for STBC single carrier CDMA transmission system based on chip-interleaved block-spread (CIBS) CDMA [17] was proposed in [18]. The structure in [18], though promising excellent performance, incurs in a relatively high computational complexity to update the equalizer coefficients [19]. In [20], time-reversal is used to provide FDE capabilities to STBC single carrier CDMA transmission system.

In this work a structure for FDE STBC CDMA-based transmission system is proposed. In this structure, transmit symbols are spread in a symbol-by-symbol basis and the self-interference in the receiver is avoided by the use of permutation matrices [21,22] in the transceiver, which also allow us to decode each transmit symbol separately. We present the proposed transmission system in a general framework, which allows us to perform an unified analysis and to present a fair comparison between commonly used CDMA-based block transmission systems. Also, as we show through computer simulations, FDE

* Correspondence: csmedina@cetuc.puc-rio.br
Centro de Estudos em Telecomunicações (CETUC), Pontifícia Universidade Católica do Rio de Janeiro (PUC-Rio), Rio de Janeiro, RJ, Brazil

algorithms used with single user detection results in a simple receiver design with good performance in terms of bit error rate (BER) when compared with previously proposed STBC CDMA transmission systems. A diversity gain analysis of the proposed transmission system is performed providing interest results.

This paper is organized as follows: Section 2 describes the baseband system model, addressing the definitions and properties of the employed matrices. In Section 3 we present and point out some properties of the receiver design, while in Section 4 different approaches for FDE are applied in the proposed scheme. Section 5 presents the results obtained through computer simulations and Section 6 gives some conclusions. A diversity and coding gain analysis is included as an appendix.

Notation. In what follows, $\boldsymbol{I}_k$ represents a $k \times k$ identity matrix, $\boldsymbol{0}_{m\times n}$, an $m \times n$ null matrix, $(\cdot)^T$, $(\cdot)^H$, $(\cdot)^*$ and $(\cdot)^\dagger$ denote transpose, Hermitian transpose, complex conjugated and Moore-Penrose matrix inverse, respectively, $\otimes$ is the Kronecker product, $\texttt{diag}(\boldsymbol{x})$ is a diagonal matrix with the components of $\boldsymbol{x}$ as its nonzero elements, $\texttt{rank}(\cdot)$ is the rank of a matrix, $\texttt{det}(\cdot)$ denotes determinant, the operator $\texttt{E}[\cdot]$ stands for ensemble average and $\mathbb{C}(\mathbb{R})$ represents the field of the complex (real) numbers.

2 System model

Consider the discrete-time equivalent baseband model of a synchronous downlink STBC CDMA system shown in Figure 1 (for convenience only one user is shown). For simplicity, in this paper we will focus on the case of two transmit antennas and one receive antenna, although this schema could be easily extended to configurations with more receive antennas, provided an appropriate combiner, such as maximal ratio combiner (MRC), would be used.

In the proposed system each of the K users transmits symbols $s_k(i) \in \mathbb{C}$, which are first spread by the M-chip spreading code $\boldsymbol{c}_k \in \mathbb{C}^M$, $||\boldsymbol{c}_k||^2 = 1$, and then grouped in vectors $\boldsymbol{c}_k s_k(i)$ of size M. It is assumed that symbols $s_k(i)$ are drawn from some constellation with zero mean and unit average symbol energy and they are independent and identically distributed (i.i.d.).

Then, the spread symbols are linearly precoded by the matrix $\boldsymbol{G} \in \mathbb{C}^{M\times M}$ and fed into the Alamouti-based space-time encoder [1] to get the space-time symbol

$$\boldsymbol{S}_k(i) = \begin{pmatrix} \bar{\boldsymbol{s}}_k(2i) & \boldsymbol{P}_{\text{tx}}\bar{\boldsymbol{s}}_k^*(2i+1) \\ \bar{\boldsymbol{s}}_k(2i+1) & -\boldsymbol{P}_{\text{tx}}\bar{\boldsymbol{s}}_k^*(2i) \end{pmatrix} \tag{1}$$

where $\bar{\boldsymbol{s}}_k(i) = \boldsymbol{G}\boldsymbol{c}_k s_k(i)$, $\boldsymbol{G}$ represents an arbitrary linear operation used to combat deleterious channel effects and to simplify equalizer designs. $\boldsymbol{P}_{\text{tx}} \in \mathbb{R}^{M\times M}$ is a permutation matrix whose design depends on the overall system and it is used to decouple, in the receiver, the transmitted symbols, as we will show later.

It should be noted that a guard interval is necessary to avoid interblock interference (IBI) in the received signal. The guard interval insertion is performed by the matrix $\boldsymbol{T} \in \mathbb{R}^{P\times M}$, where $P = M + L_{gi}$ and L_{gi} is the length of the guard interval. For the most commonly used guard intervals, cyclic prefix (CP) and zero padding (ZP), the matrix $\boldsymbol{T}$ is defined as [23]:

$$\boldsymbol{T}_{cp} = \begin{bmatrix} \boldsymbol{0}_{L_{gi}\times(M-L_{gi})} | \boldsymbol{I}_{L_{gi}} \\ \boldsymbol{I}_M \end{bmatrix} \quad \boldsymbol{T}_{zp} = \begin{bmatrix} \boldsymbol{I}_M \\ \boldsymbol{0}_{L_{gi}\times M} \end{bmatrix}.$$

The frequency-selective channel from the jth ($j = 1, 2$) transmission antenna to the receiver can be modeled

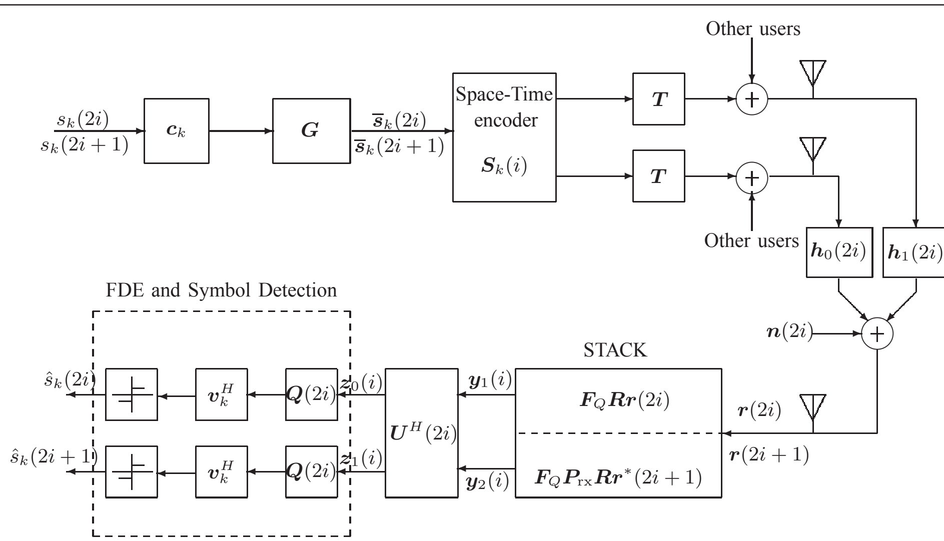

Figure 1 STBC CDMA transmission system.

using a finite-impulse response (FIR) filter with L taps, whose gains are samples, taken at the chip rate, of the equivalent baseband complex channel impulse response. Assuming that during two symbol periods the impulse response of both channels remain constant, that is, $\boldsymbol{h}_j(2i) = \boldsymbol{h}_j(2i+1) = [h_{j,0}(2i) \ldots h_{j,L-1}(2i)]^T$, $\mathbb{E}[||\boldsymbol{h}_j(2i)||^2] = 1$, the transmission through the frequency-selective MIMO channel can be represented by a $P \times P$ lower triangular Toeplitz convolution matrix $\boldsymbol{H}_j(2i)$, whose first column is $[h_{j,0}(2i) \ldots h_{j,L-1}(2i)\ 0 \ldots 0]^T$.

As we assume a downlink scenario, where the users experience the same channel condition, the received signal collected over two consecutive symbol periods is represented by the two P-dimensional vectors:

$$\begin{aligned} \boldsymbol{r}(2i) &= \boldsymbol{H}_0(2i)\boldsymbol{T}\bar{\boldsymbol{s}}(2i) \\ &\quad + \boldsymbol{H}_1(2i)\boldsymbol{T}\bar{\boldsymbol{s}}(2i+1) + \boldsymbol{n}(2i) + \boldsymbol{\eta}(2i) \\ \boldsymbol{r}(2i+1) &= \boldsymbol{H}_0(2i)\boldsymbol{T}\boldsymbol{P}_{2\mathrm{tx}}\bar{\boldsymbol{s}}^*(2i+1) \\ &\quad - \boldsymbol{H}_1(2i)\boldsymbol{T}\boldsymbol{P}_{\mathrm{tx}}\bar{\boldsymbol{s}}^*(2i) + \boldsymbol{n}(2i+1) \\ &\quad + \boldsymbol{\eta}(2i+1) \end{aligned} \tag{2}$$

where $\boldsymbol{n}(i)$ is a complex white Gaussian noise vector with zero mean and covariance matrix $\mathbb{E}[\boldsymbol{n}(i)\boldsymbol{n}^H(i)] = N_0\boldsymbol{I}_P$, N_0 is the noise spectral density, $\boldsymbol{\eta}(i)$ denotes the IBI present in non-ZP systems ($\boldsymbol{\eta}(i) = \boldsymbol{0}$ in ZP systems) and

$$\bar{\boldsymbol{s}}(i) = \sqrt{\tilde{E}_s}\sum_{k=1}^{K}\rho_k\bar{\boldsymbol{s}}_k(i) = \sqrt{\tilde{E}_s}\boldsymbol{G}\boldsymbol{C}\boldsymbol{\rho}\boldsymbol{s}(i) \tag{3}$$

where $\tilde{E}_s = (E_1 + \cdots + E_K)/K$ is the mean received energy, with E_k being the energy of the k user signal, $\rho_k = \sqrt{E_k/2\tilde{E}_s}$, $\boldsymbol{\rho} = \mathtt{diag}(\rho_1; \ldots \rho_K)$, $\boldsymbol{C} = [\boldsymbol{c}_1 \cdots \boldsymbol{c}_K]$, $\boldsymbol{s}(i) = [s_1(i) \ldots s_K(i)]^{\mathrm{T}}$.

If CP is used as guard interval at the transmitter, the receiver must remove the guard interval from the received signal to eliminate IBI. If ZP is used at the transmitter the IBI is null, and then, the guard interval removal is not necessary. This operation is represented by the matrix $\boldsymbol{R}$, where $\boldsymbol{R} = \boldsymbol{R}_{cp} = [\boldsymbol{0}_{M\times L_{gi}}|\boldsymbol{I}_M]$ for CP systems and $\boldsymbol{R} = \boldsymbol{R}_{zp} = \boldsymbol{I}_P$ for ZP systems.

Finally, the space-time decoding is performed by first stacking the received signals over two consecutive symbol periods, as:

$$\boldsymbol{y}(i) = \begin{bmatrix} \boldsymbol{F}_Q\boldsymbol{R}\boldsymbol{r}(2i) \\ \boldsymbol{F}_Q\boldsymbol{P}_{\mathrm{rx}}\boldsymbol{R}\boldsymbol{r}^*(2i+1) \end{bmatrix} \tag{4}$$

where $Q = M$ for CP systems and $Q = P$ for ZP case, $\boldsymbol{P}_{\mathrm{rx}} \in \mathbb{R}^{Q\times Q}$ is a permutation matrix whose design depends on the overall system, and in conjunction with $\boldsymbol{P}_{\mathrm{tx}}$ it is used to perform symbol decoupling in the received STBC symbols, as will be detailed below. $\boldsymbol{F}_Q$ is a $Q \times Q$ matrix that implements a Q-point discrete Fourier transform, normalized such that, $\boldsymbol{F}_Q^H\boldsymbol{F}_Q = \boldsymbol{F}_Q\boldsymbol{F}_Q^H = \boldsymbol{I}_Q$.

Using (2) and (3), we can rewrite (4) as

$$\boldsymbol{y}(i) = \begin{bmatrix} \boldsymbol{f}_0(\boldsymbol{H}_0)\boldsymbol{s}(2i) + \boldsymbol{f}_0(\boldsymbol{H}_1)\boldsymbol{s}(2i+1) \\ \boldsymbol{f}_1(\boldsymbol{H}_0)\boldsymbol{s}(2i+1) - \boldsymbol{f}_1(\boldsymbol{H}_1)\boldsymbol{s}(2i) \end{bmatrix} + \underbrace{\begin{bmatrix} \boldsymbol{F}_Q\boldsymbol{R}\boldsymbol{n}(2i) \\ \boldsymbol{F}_Q\boldsymbol{P}_{\mathrm{rx}}\boldsymbol{R}\boldsymbol{n}*(2i+1) \end{bmatrix}}_{\bar{n}(i)} \tag{5}$$

where

$$\boldsymbol{f}_0(\boldsymbol{H}_j) = \sqrt{\tilde{E}_s}\boldsymbol{F}_Q\boldsymbol{R}\boldsymbol{H}_j(2i)\boldsymbol{T}\boldsymbol{G}\boldsymbol{C}\boldsymbol{\rho} \tag{6}$$

$$\boldsymbol{f}_1(\boldsymbol{H}_j) = \sqrt{\tilde{E}_s}\boldsymbol{F}_Q\boldsymbol{P}_{\mathrm{rx}}\boldsymbol{R}\boldsymbol{H}_j^*(2i)\boldsymbol{T}\boldsymbol{P}_{\mathrm{tx}}\boldsymbol{G}\boldsymbol{C}\boldsymbol{\rho}. \tag{7}$$

Note that the term $\boldsymbol{\eta}(i)$ in (2), which accounts for IBI in non-ZP guard interval systems, is removed by the joint operation of matrices $\boldsymbol{T}$ and $\boldsymbol{R}$. It should be stressed that the guard interval length must be at least the channel order in order to avoid IBI, i.e., $L_{gi} \geq L - 1$ [23].

The choice of ZP or CP as the guard interval is convenient, since it allows us the use of the following well known properties:

(p1) CP case: $\boldsymbol{R}_{cp}\boldsymbol{H}_j(2i)\boldsymbol{T}_{cp}$ reduces to a circulant matrix, $\mathbb{H}_j(2i)$, of dimension $M \times M$.

(p2) ZP case: $\boldsymbol{R}_{zp}\boldsymbol{H}_j(2i)\boldsymbol{T}_{zp}$ is equivalent to $\mathbb{H}_j(2i)\boldsymbol{T}_{zp}$ where $\mathbb{H}_j(2i)$ is a circulant matrix of dimension $P \times P$. The equivalence is due to $\boldsymbol{R}_{zp} = \boldsymbol{I}_P$ and the structure of $\boldsymbol{T}_{zp}$.

(p3) A circulant matrix $\mathbb{H}_j(2i)$ of dimension $Q \times Q$, as in (p1) and (p2), can be decomposed as $\mathbb{H}_j(2i) = \boldsymbol{F}_Q^H\boldsymbol{\Lambda}_j(2i)\boldsymbol{F}_Q$ and $\mathbb{H}_j^H(2i) = \boldsymbol{F}_Q^H\boldsymbol{\Lambda}_j^*(2i)\boldsymbol{F}_Q$, where $\boldsymbol{\Lambda}_j(2i)$ is a diagonal matrix whose entries are the frequency response of the transmission channel $\boldsymbol{h}_j(2i)$, i.e., $\boldsymbol{\Lambda}_j(2i) = \mathtt{diag}(\tilde{\boldsymbol{F}}_{Q\times L}\boldsymbol{h}_j(2i))$, where $\tilde{\boldsymbol{F}}_{Q\times L}$ is a $Q \times L$ matrix formed with the first L columns of the matrix that implements the (non-normalized) Q-point discrete Fourier transform.

In order to decouple the transmitted symbols and to provide FDE capabilities to the system, we choose $\boldsymbol{P}_{\mathrm{tx}}$ and $\boldsymbol{P}_{\mathrm{rx}}$ as in [21], where they are drawn from a set $\{\boldsymbol{P}_J^{(n)}\}_{n=0}^{J-1}$, where J is the dimension of $\boldsymbol{P}$. Each $\boldsymbol{P}_J^{(n)}$ performs a reverse cyclic shift that depends on n when applied to a $J \times 1$ vector. This set of matrices has two useful properties:

(p4) Pre- and post-multiplying a circulant matrix, $\mathbb{H}_j(2i)$, by $\boldsymbol{P}_J^{(n)}$ yields $H_j^{\mathrm{T}}(2i)$, i.e., $\boldsymbol{P}_J^{(n)}H_j(2i)\boldsymbol{P}_J^{(n)} = \mathbb{H}_j^{\mathrm{T}}(2i)$ and $\boldsymbol{P}_J^{(n)}\mathbb{H}_j^*(2i)\boldsymbol{P}_J^{(n)} = \mathbb{H}_j^H(2i)$[21].

(p5) $\boldsymbol{T}_{zp}\boldsymbol{P}_M^{(0)} = \boldsymbol{P}_P^{(M)}\boldsymbol{T}_{zp}$[22].

Then, if for CP systems we choose $\boldsymbol{P}_{\text{rx}} = \boldsymbol{P}_{\text{tx}} = \boldsymbol{P}_M^{(0)}$ and using (p1), (p4) and (p3) we get:

$$f_0(\boldsymbol{H}_j) = \sqrt{\tilde{E}_s}\boldsymbol{\Lambda}_j(2i)\boldsymbol{F}_M\boldsymbol{G}\boldsymbol{C}\boldsymbol{\rho} = \sqrt{\tilde{E}_s}\boldsymbol{\Lambda}_j(2i)\boldsymbol{V} \tag{8}$$

$$f_1(\boldsymbol{H}_j) = \sqrt{\tilde{E}_s}\boldsymbol{\Lambda}_j^*(2i)\boldsymbol{F}_M\boldsymbol{G}\boldsymbol{C}\boldsymbol{\rho} = \sqrt{\tilde{E}_s}\boldsymbol{\Lambda}_j^*(2i)\boldsymbol{V} \tag{9}$$

where $\boldsymbol{V} = \boldsymbol{F}_M\boldsymbol{G}\boldsymbol{C}\boldsymbol{\rho}$.

In the same way, for ZP systems we can choose $\boldsymbol{P}_{\text{rx}} = \boldsymbol{P}_P^{(M)}$ and $\boldsymbol{P}_{\text{tx}} = \boldsymbol{P}_M^{(0)}$, then using (p2), (p5), (p4) and (p3) we have:

$$f_0(\boldsymbol{H}_j) = \sqrt{\tilde{E}_s}\boldsymbol{\Lambda}_j(2i)\boldsymbol{F}_P\boldsymbol{T}_{zp}\boldsymbol{G}\boldsymbol{C}\boldsymbol{\rho} = \sqrt{\tilde{E}_s}\boldsymbol{\Lambda}_j(2i)\boldsymbol{V} \tag{10}$$

$$f_1(\boldsymbol{H}_j) = \sqrt{\tilde{E}_s}\boldsymbol{\Lambda}_j^*(2i)\boldsymbol{F}_P\boldsymbol{T}_{zp}\boldsymbol{G}\boldsymbol{C}\boldsymbol{\rho} = \sqrt{\tilde{E}_s}\boldsymbol{\Lambda}_j^*(2i)\boldsymbol{V} \tag{11}$$

where $\boldsymbol{V} = \boldsymbol{F}_P\boldsymbol{T}_{zp}\boldsymbol{G}\boldsymbol{C}\boldsymbol{\rho}$.

Now, using the results (8)-(11), the space-time decoded vector in (5), can be expressed as

$$\boldsymbol{\gamma}(i) = \sqrt{\tilde{E}_s}\underbrace{\begin{bmatrix} \boldsymbol{\Lambda}_0(2i) & \boldsymbol{\Lambda}_1(2i) \\ -\boldsymbol{\Lambda}_1^*(2i) & \boldsymbol{\Lambda}_0^*(2i) \end{bmatrix}}_{\boldsymbol{\Lambda}(2i)}\begin{bmatrix} \boldsymbol{V}\,\boldsymbol{s}(2i) \\ \boldsymbol{V}\,\boldsymbol{s}(2i+1) \end{bmatrix} + \bar{\boldsymbol{n}}(i) \tag{12}$$

where $\boldsymbol{\Lambda}_j(2i) = \texttt{diag}(\tilde{\boldsymbol{F}}_{Q\times L}\boldsymbol{h}_j(2i))$ $(j = 0, 1)$ and $\boldsymbol{V}$ is the $Q \times K$ matrix defined in connection with (8)-(11).

Note that the noise vector $\bar{\boldsymbol{n}}(i)$ in (5) and (12) is still Gaussian with zero mean and covariance matrix $N_0\boldsymbol{I}_{2Q}$.

3 Receiver Design

Assuming that perfect channel estimation is performed at the receiver, we can define an orthogonal matrix $\boldsymbol{U}(2i) = \boldsymbol{\Lambda}(2i)(\boldsymbol{I}_2 \otimes \boldsymbol{\Lambda}_{01}^{-1}(2i))$ of dimension $2Q \times 2Q$, where

$$\boldsymbol{\Lambda}_{01}(2i) = [\boldsymbol{\Lambda}_0^*(2i)\boldsymbol{\Lambda}_0(2i) + \boldsymbol{\Lambda}_1^*(2i)\boldsymbol{\Lambda}_1(2i)]^{1/2}. \tag{13}$$

Then, $\boldsymbol{U}^H(2i)\boldsymbol{\Lambda}(2i) = \boldsymbol{I}_2 \otimes \boldsymbol{\Lambda}_{01}(2i)$, and

$$\boldsymbol{z}(i) = \boldsymbol{U}^H(2i)\boldsymbol{\gamma}(i) = \sqrt{\tilde{E}_s}\begin{bmatrix} \boldsymbol{\Lambda}_{01}(2i) & \boldsymbol{0}_{Q\times Q} \\ \boldsymbol{0}_{Q\times Q} & \boldsymbol{\Lambda}_{01}(2i) \end{bmatrix} \cdot \begin{bmatrix} \boldsymbol{V}\,\boldsymbol{s}(2i) \\ \boldsymbol{V}\,\boldsymbol{s}(2i+1) \end{bmatrix} + \boldsymbol{U}^H(2i)\bar{\boldsymbol{n}}(i) \tag{14}$$

thus, $\boldsymbol{U}(2i)$ decouples the received vector allowing $\boldsymbol{s}(2i)$ and $\boldsymbol{s}(2i+1)$ to be demodulated separately from:

$$\begin{aligned} \boldsymbol{z}_0(i) &= \sqrt{\tilde{E}_s}\boldsymbol{\Lambda}_{01}(2i)\boldsymbol{V}\,\boldsymbol{s}(2i) + \bar{\boldsymbol{n}}_0(2i) \\ \boldsymbol{z}_1(i) &= \sqrt{\tilde{E}_s}\boldsymbol{\Lambda}_{01}(2i)\boldsymbol{V}\boldsymbol{s}(2i+1) + \bar{\boldsymbol{n}}_1(2i+1) \end{aligned} \tag{15}$$

where $\boldsymbol{U}^H(2i)\bar{\boldsymbol{n}}(i) = [\bar{\boldsymbol{n}}_0^T(2i) \quad \bar{\boldsymbol{n}}_1^T(2i+1)]^{\text{T}}$. As $\boldsymbol{U}(2i)$ is an orthogonal matrix, it does not alter the statistical properties of the noise vector $\bar{\boldsymbol{n}}(i)$.

With $\boldsymbol{z}_j(i)$ $(j = 0, 1)$, as in (15), symbol detection can adopt different approaches as illustrated next.

3.1 Multiuser maximum likelihood (ML) detection

The optimal solution of the proposed system is to jointly detect the transmitted symbol of the different users within the transmitted vector, based on the received vector. Thus, the optimum receiver is a multiuser (MU) maximum likelihood (ML) receiver, implemented, in this case, by the minimum distance receiver, such that, for $j = 0, 1$:

$$\hat{\boldsymbol{s}}(2i+j) = \arg\min_{\boldsymbol{s}} \left\| \sqrt{\tilde{E}_s}\boldsymbol{\Lambda}_{01}(2i)\boldsymbol{V}\,\boldsymbol{s} - \boldsymbol{z}_j(i) \right\|^2. \tag{16}$$

As shown in the appendix, the maximum diversity gain $G_d = 2L$, is attained for this receiver when $||\boldsymbol{\Lambda}_{01}(2i)\boldsymbol{V}\boldsymbol{e}||^2 \neq 0$, $\forall \boldsymbol{e} \neq \boldsymbol{0}$. Then, a sufficient condition for maximum diversity gain, is to guarantee that, for any $\boldsymbol{e} \neq \boldsymbol{0}$, at least L elements from $\boldsymbol{V}\boldsymbol{e}$ are different from zero.

Proof: In the following, we drop the time index to simplify the notation. Let $\lambda_{01,l}$ be the real and non-negative lth element of the diagonal of Λ_{01} and e_l' the lth element of $\boldsymbol{V}\boldsymbol{e}$, then:

$$||\boldsymbol{\Lambda}_{01}\boldsymbol{V}\,\boldsymbol{e}||^2 = \sum_{l=0}^{Q-1} \lambda_{01,l}^2 |e'_l|^2 \tag{17}$$

where $\lambda_{01,l}^2 = |\lambda_{0,l}|^2 + |\lambda_{1,l}|^2$, with $\lambda_{j,l}$ $(j = 0, 1)$ being the l-th element of $\tilde{\boldsymbol{F}}_{Q\times L}\boldsymbol{h}_j (j = 0, 1)$. Since the Q-points discrete Fourier transform of a vector of size L can have at most L - 1 zero elements, it then results that at most L - 1 values of $\lambda_{01,l}$ can be equal to zero. Then, if $e_l' = \boldsymbol{V}\,\boldsymbol{e}$ has at least L elements different from zero, we have that $\sum_{l=0}^{Q-1} \lambda_{01,l}^2 |e_l'|^2 \neq 0$ and the maximum diversity gain is achieved. ■

3.1.1 ZP systems

For the ZP systems, $\boldsymbol{V} = \boldsymbol{F}_P\boldsymbol{T}_{zp}\boldsymbol{G}\boldsymbol{C}\boldsymbol{\rho}$. Now using $\boldsymbol{V}\,\boldsymbol{e} = \tilde{\boldsymbol{F}}_{P\times M}\boldsymbol{e}_0$, where $\tilde{\boldsymbol{F}}_{P\times M} = \boldsymbol{F}_P\boldsymbol{T}_{zp}$ is $P \times M$ matrix formed with the first M columns of $\boldsymbol{F}_P$ and $\boldsymbol{e}_0 = \boldsymbol{G}\boldsymbol{C}\boldsymbol{\rho}\boldsymbol{e}$ is a M-dimensional vector, if the user codes are linearly independent, and provided that $\boldsymbol{G}$ is non-singular, then $\boldsymbol{G}\boldsymbol{C}$ is full column rank and therefore $\boldsymbol{e}_0 \neq \boldsymbol{0}$ for any $\boldsymbol{e} \neq \boldsymbol{0}$. Again, since the P-points discrete Fourier transform of a sequence of M points can have at most M - 1 zeros, then $\tilde{\boldsymbol{F}}_{P\times M}\boldsymbol{e}_0$ has at least P - (M - 1) = L + 1 elements different from zero, thus maximum diversity gain is achieved.

So, for ZP systems, the maximum diversity gain is achieved independent of the choice of the user codes, the precoding matrix and the number of users on the system, provided that $\boldsymbol{GC}$ is full column rank.

3.1.2 CP systems

For CP systems $\boldsymbol{V} = \boldsymbol{F}_M\boldsymbol{GC\rho}$, then, in general, we cannot guarantee that the maximum diversity gain is achieved by the system. However, proper choices of the precoding matrix and spreading codes, can lead to full diversity gain. For example, if $\boldsymbol{F}_M\boldsymbol{GC}$ is a Vandermonde matrix (e.g., $\boldsymbol{G} = \boldsymbol{F}_M^H$ and the codes $\boldsymbol{c}_k$ are columns of a Vandermonde matrix[1]), and $\boldsymbol{GC}$ is full column rank, then for any K dimensional vector $\boldsymbol{e} \neq \boldsymbol{0}$, $\boldsymbol{Ve}$ has at most K - 1 zeroes, or equivalently, it has at least M - K + 1 elements different from zero. Then, maximum diversity gain is achieved provided that $K \leq M - L + 1$.

3.2 Minimum mean squared error single user detection

Using $\boldsymbol{z}_j(i)$ (j = 0, 1), from (15), the kth user minimum mean squared error (MMSE) receiver for each symbol, $\boldsymbol{w}_{k,j}$, is obtained by minimizing the mean-squared error criterion

$$\boldsymbol{w}_{k,j} = \arg\min_{\boldsymbol{w}} \mathrm{E}\left[|s_k(2i+j) - \boldsymbol{w}^H\boldsymbol{z}_j(i)|^2\right], \tag{18}$$

whose solution is given by [24]:

$$\boldsymbol{w}_{k,j} = \boldsymbol{R}_{\boldsymbol{z}_j\boldsymbol{z}_j}^{-1}\boldsymbol{p}_{\boldsymbol{z}_j s_k}, \tag{19}$$

where $\boldsymbol{R}_{\boldsymbol{z}_j\boldsymbol{z}_j} = \mathrm{E}\left[\boldsymbol{z}_j(i)\boldsymbol{z}_j^H(i)\right]$ and $\boldsymbol{p}_{\boldsymbol{z}_j s_k} = \mathrm{E}[\boldsymbol{z}(i)s_k^*(2i+j)]$.

Symbol detection is performed for j = 0, 1 as:

$$\hat{s}_k(2i+j) = \mathtt{disc}\left\{\boldsymbol{w}_{k,j}^H\boldsymbol{z}_j(i)\right\} \tag{20}$$

where $\mathtt{disc}\{n\}$ returns the symbol constellation closer to n.

From (15) is easy to conclude that

$$\boldsymbol{R}_{\boldsymbol{z}_0\boldsymbol{z}_0} = \boldsymbol{R}_{\boldsymbol{z}_1\boldsymbol{z}_1} = \tilde{E}_s\boldsymbol{\Lambda}_{01}(2i)\boldsymbol{V}\boldsymbol{V}^H\boldsymbol{\Lambda}_{01}^H(2i) + N_0\boldsymbol{I}_Q \tag{21}$$

and $\boldsymbol{p}_{\boldsymbol{z}_0 s_k} = \boldsymbol{p}_{\boldsymbol{z}_1 s_k} = \tilde{E}_s\boldsymbol{\Lambda}_{01}(2i)\boldsymbol{v}_k$, where $\boldsymbol{v}_k$ is the kth column of $\boldsymbol{V}$. It follows that $\boldsymbol{w}_{k,0} = \boldsymbol{w}_{k,1}$.

As we assume downlink transmission, in practical situations only the kth column of $\boldsymbol{V}$ is known to the kth user receiver. Then, an iterative procedure, like the recursive least squares (RLS) algorithm [24] or conjugated gradient algorithm [25], must be used to compute the desired solution (19).

4 Frequency domain equalization

From (15) one can see that FDE can be performed by applying an one-tap chip-equalizer to each component of the vectors $\boldsymbol{z}_j(i)$ (j = 0, 1). Such operation is represented by the pre-multiplication of the vectors $\boldsymbol{z}_j(i)$ (j = 0, 1) by a diagonal matrix $\boldsymbol{Q}(2i) \in \mathbb{C}^{Q\times Q}$, whose elements are the weights of the one-tap chip-equalizer.

Symbol detection is then performed over the frequency equalized and despread signal:

$$\hat{\boldsymbol{s}}(2i+j) = \mathtt{disc}\left\{\boldsymbol{V}^\dagger\boldsymbol{Q}(2i)\boldsymbol{z}_j(i)\right\} \quad j = 0, 1 \tag{22}$$

where $\mathtt{disc}\{\boldsymbol{n}\}$ is the vector whose components are the symbols of the signal constellation closer to the components of vector $\boldsymbol{n}$ and $(\cdot)^\dagger$ represent the Moore-Penrose matrix inverse. In order to avoid high computational complexity algorithms, it is desired to have $\boldsymbol{V}^\dagger = \boldsymbol{V}^H$, which is true, for example, if $\boldsymbol{G}$ is an orthogonal matrix and the spreading codes are orthogonal.

As in the downlink the receiver is only interested in the kth user, symbol detection is performed as

$$\hat{s}_k(2i+j) = \mathtt{disc}\left\{\boldsymbol{v}_k^H\boldsymbol{Q}(2i)\boldsymbol{z}_j(i)\right\} \tag{23}$$

where $\boldsymbol{v}_k$ is the kth column of $\boldsymbol{V}$, and we assume that $\boldsymbol{V}^\dagger = \boldsymbol{V}^H$.

Now, let us consider the noiseless part of the decision variable, $\boldsymbol{v}_k^H\boldsymbol{Q}(2i)\boldsymbol{z}_j(i)$. For the CP case we have

$$\boldsymbol{c}_k^H\boldsymbol{G}^H\underbrace{\boldsymbol{F}_M^H\tilde{\boldsymbol{I}}(2i)\boldsymbol{F}_M}_{\tilde{\mathbb{I}}_{CP}(2i)}\boldsymbol{GC}\,\boldsymbol{s}(2i+j) \tag{24}$$

and for the ZP case

$$\boldsymbol{c}_k^H\boldsymbol{G}^H\boldsymbol{T}_{zp}^H\underbrace{\boldsymbol{F}_P^H\tilde{\boldsymbol{I}}(2i)\boldsymbol{F}_P}_{\tilde{\mathbb{I}}_{ZP}(2i)}\boldsymbol{T}_{zp}\boldsymbol{GC}\,\boldsymbol{s}(2i+j) \tag{25}$$

where $\tilde{\boldsymbol{I}}(2i) = \boldsymbol{Q}(2i)\boldsymbol{\Lambda}_{01}(2i)$ is a diagonal matrix. Note that in general $\tilde{\boldsymbol{I}}(2i) \neq \boldsymbol{I}_Q$, and thus $\tilde{\mathbb{I}}_{CP}(2i) = \boldsymbol{F}_M^H\tilde{\boldsymbol{I}}(2i)\boldsymbol{F}_M$ and $\tilde{\mathbb{I}}_{ZP}(2i) = \boldsymbol{F}_P^H\tilde{\boldsymbol{I}}(2i)\boldsymbol{F}_P$ are circulant matrices that introduce code distortion and inter-chip interference in the equalization process.

So, one can design the precoding matrix, $\boldsymbol{G}$, in order to mitigate such undesired effects. Two simple approaches are commonly used. The first one is to choose the identity matrix as the precoding matrix, resulting into the well-known single-carrier block transmission systems. In both cases, CP and ZP systems, single carrier modulation presents code distortion and inter-chip interference, produced by the circulant matrix $\tilde{\mathbb{I}}(2i)$.

The second approach is to choose $\boldsymbol{G} = \boldsymbol{F}_M^H$, leading the so-called multicarrier block transmission systems. In this case, for CP systems, the noiseless decision variable (24) reduces to $\boldsymbol{c}_k^H\tilde{\boldsymbol{I}}(2i)\boldsymbol{C}\,\boldsymbol{s}(2i+j)$, that states the absence of inter-chip interference (as $\tilde{\boldsymbol{I}}(2i)$ is a diagonal matrix), however, code distortion is present.

We next consider the design of the one-tap equalization matrix $\boldsymbol{Q}(2i) = \mathtt{diag}(q_0(2i),\ldots, q_Q(2i))$ following standard approaches.

4.1 MRC single user detection

This receiver weights each sub-channel by its respective complex conjugate equivalent sub-channel coefficient, leading in the present case to

$$q_l(2i) = \lambda_{01,l}(2i) = \sqrt{|\lambda_{0,l}(2i)|^2 + |\lambda_{1,l}(2i)|^2} \quad (26)$$

where $\lambda_{01,l}(2i)$ is the real and non-negative lth element of the diagonal of $\boldsymbol{\Lambda}_{01}(2i)$ and $\lambda_{j,l}(2i)$ (j = 0, 1) is the lth element of $\tilde{\boldsymbol{F}}_{Q\times L}\boldsymbol{h}_j(2i)$.

Whit this choice, $\boldsymbol{Q}(2i) = \boldsymbol{\Lambda}_{01}(2i)$ and then $\tilde{\boldsymbol{I}}(2i) = \boldsymbol{\Lambda}_{01}^2(2i)$. Thus, this equalize the spreading code distortion introduced by the transmission channel and may enhance the multiple access interference (MAI).

4.2 Zero forcing (ZF) single-user receiver

Zero forcing applies channel inversion so that $\boldsymbol{Q}(2i) = \boldsymbol{\Lambda}_{01}^{-1}(2i)$ and $\tilde{\boldsymbol{I}}(2i) = \boldsymbol{I}_Q$. Thus, this equalizer eliminates code distortion, and for the case of multicarrier with CP transmissions systems also removes the inter-chip interference and can, therefore, eliminate MAI (if user codes are orthogonal). The equalizer coefficients are chosen as

$$q_l(2i) = \frac{1}{\lambda_{01,l}(2i)}. \quad (27)$$

The main drawback of this equalizer is that when $\lambda_{01,l}(2i) \approx 0$, the noise effects are enhanced.

4.3 MMSE single-user detection

The equalization coefficient based on the MMSE criterion for the proposed system results in [26]:

$$q_l(2i) = \frac{\lambda_{01,l}(2i)}{\lambda_{01,l}^2(2i) + \sigma^2} \quad (28)$$

where σ^2 is the variance of the noise. We have $\boldsymbol{Q}(2i) = (\boldsymbol{\Lambda}_{01}^2(2i) + \sigma^2\boldsymbol{I})^{-1}\boldsymbol{\Lambda}_{01}(2i)$ and $\tilde{\boldsymbol{I}}(2i) = (\boldsymbol{\Lambda}_{01}^2(2i) + \sigma^2\boldsymbol{I})^{-1}\boldsymbol{\Lambda}_{01}^2(2i)$, thus, as with the MRC this equalizer does not eliminate code distortion. However, it offers a good trade off between code distortion reduction and noise enhancement.

5 Simulation results

We consider the downlink scenario of the proposed STBC CDMA transmission system with two transmit and one receive antenna. The data symbols are binary phase-shift keying (BPSK) modulated and spreading by a length M = 16 spreading code. The system is loaded with K = 4 users and two types of guard intervals are considered in combination with two different choices of precoding matrix, $\boldsymbol{G} = \boldsymbol{I}_M$ and $\boldsymbol{G} = \boldsymbol{F}_M^H$, leading to four different systems, as shown in Table 1 where MC stands for multicarrier and SC for single carrier.

In all the experiments, we obtain the average bit-error rate (BER) versus E_b/N_0 (E_b is the energy per bit of the desired user) as the performance measure. In each experiment we run 30, 000 Monte Carlo realizations, with 2,000 symbols transmitted per run. The transmitted symbols are randomly generated and it is assumed that the first 500 symbols are used as the train sequence for the equalizers.

5.1 Performance of the transceiver

In the first experiment we compare two different transceivers, the one proposed in [4], adapted to the systems in Table 1 as reported in [16], denoted as STBC in the figures, and the transceiver proposed in this work. In order to allow a fair comparison between the transceivers, we employ a MMSE type of receiver (see Section 3.2), with a conjugated gradient [25] adaptive implementation. For comparison purposes, the performance of a single user MMSE type of receiver for a block CDMA-based system with only one antenna at the transmitter and one antenna at the receiver, denoted as SISO, is also presented.

The channel from each transmit antenna to the receiver is modeled here as a time-variant FIR filter, with coefficients given by $h_{j,l}(i) = p_{j,l}\alpha_{j,l}(i)$ (j = 1, 2 and l = 0, 1, 2,..., L - 1) where $\alpha_{j,l}(i)$ is obtained with Clarke's model [27]. This procedure corresponds to the generation of independent sequences of correlated unit power complex Gaussian random variables ($\mathrm{E}\left[|\alpha_{j,l}^2(i)|\right] = 1$) with the path weights $p_{j,l}$ normalized so that $\sum_{l=0}^{L-1}|p_{j,l}|^2 = 1$. Here, the channel coefficients are kept constant during two-symbol period and each channel has L = 4 transmission paths of equal weight, i.e., $|p_{j,l}|^2 = 1/L$, l = 0, 1, 2, 3. The guard interval length is L_{gi} = 3. The results depend on the normalized Doppler frequency (f_dT), where f_d is the Doppler frequency and T is the duration of two symbols. A value f_dT = 0.001 was assumed in all simulations. The systems use Hadamard codes of length M = 16. In each run, the user codes were randomly chosen, but we avoid the use of the first and second Hadamard code, which corresponds to the first and second column of the Hadamard matrix.

Table 1 Transmission system considered

Transmission System	G	T	R
MC CDMA CP	$\boldsymbol{F}_M^H$	$\boldsymbol{T}_{cp}$	$\boldsymbol{R}_{cp}$
MC CDMA ZP	$\boldsymbol{F}_M^H$	$\boldsymbol{T}_{zp}$	$\boldsymbol{I}_P$
SC CDMA CP	$\boldsymbol{I}_M$	$\boldsymbol{T}_{cp}$	$\boldsymbol{R}_{cp}$
SC CDMA ZP	$\boldsymbol{I}_M$	$\boldsymbol{T}_{zp}$	$\boldsymbol{I}_P$

For the proposed transceiver, before the MMSE single user detection stage, decoupling of the received vector must be performed, as shown in (14), (15). For this purpose, two channel estimates were used. The first one is an ideally estimated channel, denoted as Proposed in the figures, while the second one, denoted 'Proposed w/ Error' in the figures, is a noisy channel estimate, $\hat{\boldsymbol{h}}_j(2i) = \boldsymbol{h}_j(2i) + \boldsymbol{\zeta}_j(2i)$, where $\zeta_j(2i)$ is a complex white Gaussian noise vector with zero mean and covariance matrix $\mathrm{E}\left[\boldsymbol{\zeta}_j(2i)\boldsymbol{\zeta}_j^H(2i)\right] = \sigma_\zeta^2 \boldsymbol{I}_L$. In this experiment, we set the mean squared relative error of the channel estimate to 10 dB. Note, that the conjugated gradient algorithm that follows the decoupling does not need the channel knowledge to reach the MMSE solution.

Figures 2 and 3 show the BER results versus E_b/N_0 for CP and ZP systems, respectively. As can be noted, for multicarrier systems, the proposed receiver performs better than the STBC receiver, even in the presence of channel estimation errors. When comparing multicarrier systems versus single carrier systems, we observe the BER floor for single carrier systems. This is due, in part, to the better recovering of the spreading codes performed by the multicarrier systems.

In the case of SC CDMA ZP system of the Figure 3, it was observed that the receiver restored some of the orthogonality between user codes, resulting in good signal to interference-plus-noise ratio, which in turn results in enhanced BER. For the case of SC CDMA CP of the Figure 2, the same receiver could not restore the orthogonality between user codes, resulting in poor signal to interference-plus-noise ratio and then in worst BER.

5.2 Performance of FDE algorithms

In this experiment we compare different FDE algorithms for the proposed structure (see Section 4): MRC single user receiver (FDE MRC), zero forcing single user receiver (FDE ZF), and MMSE single user receiver (FDE MMSE). We use the same time-variant channel used in the first experiment and we assume that the channel was perfectly estimated. The system uses Hadamard codes of length M = 16 and were chosen as in the first experiment. Results for a matched filter single user algorithm (MF) are also shown in the figures. In this algorithm the receiver filter is matched to the user spreading code at the receiver.

Figures 4 and 5 show the BER results versus E_b/N_0 for CP and ZP systems, respectively. As expected, the FDE MMSE receiver outperforms the FDE ZF, the FDE MRC and the MF receivers. Furthermore, all these receivers have similar computational complexity.

Also note that for FDE ZF and FDE MMSE receivers, multicarrier systems perform better than for single carrier systems due to the small and even null inter-chip interference of multicarrier systems with FDE, as stated before in Section 4.

5.3 Performance with different channel covariance matrix

In the third experiment we compare the performance of the systems for three different transmission channels, all with L = 4 paths but different channel covariance matrices.

The process to generate the time-variant channel for each user is as in the first experiment. The first channel assumes uncorrelated transmission paths of equal weight, i.e., $|p_{j,l}|^2 = 1/L$, j = 1, 2 and l = 0, 1, 2, 3, as in

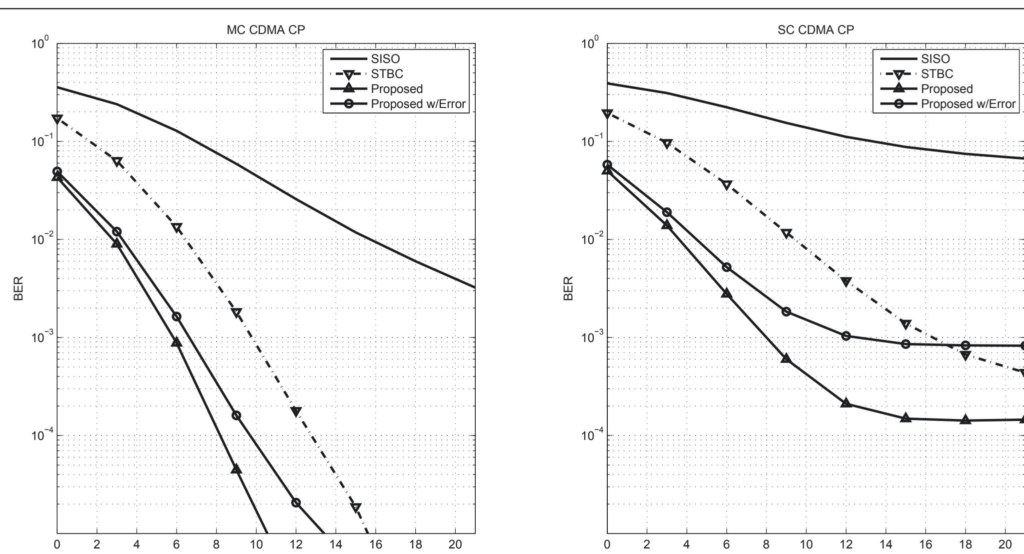

Figure 2 Performance of the transceiver. **(a)** BER versus E_b/N_0 for CP systems. **(b)** BER versus E_b/N_0 for ZP systems.

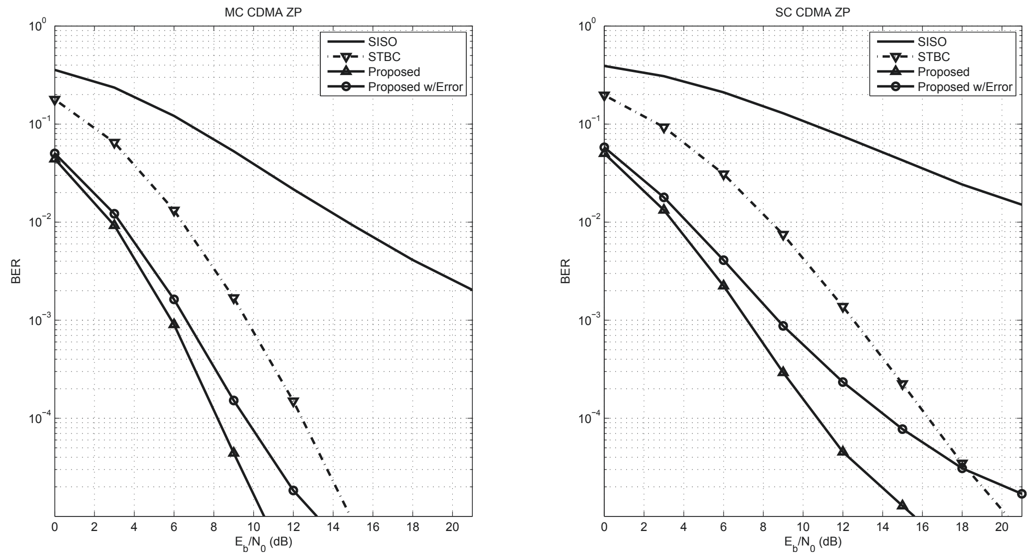

Figure 3 Performance of the transceiver. BER versus E_b/N_0 for zero padding systems.

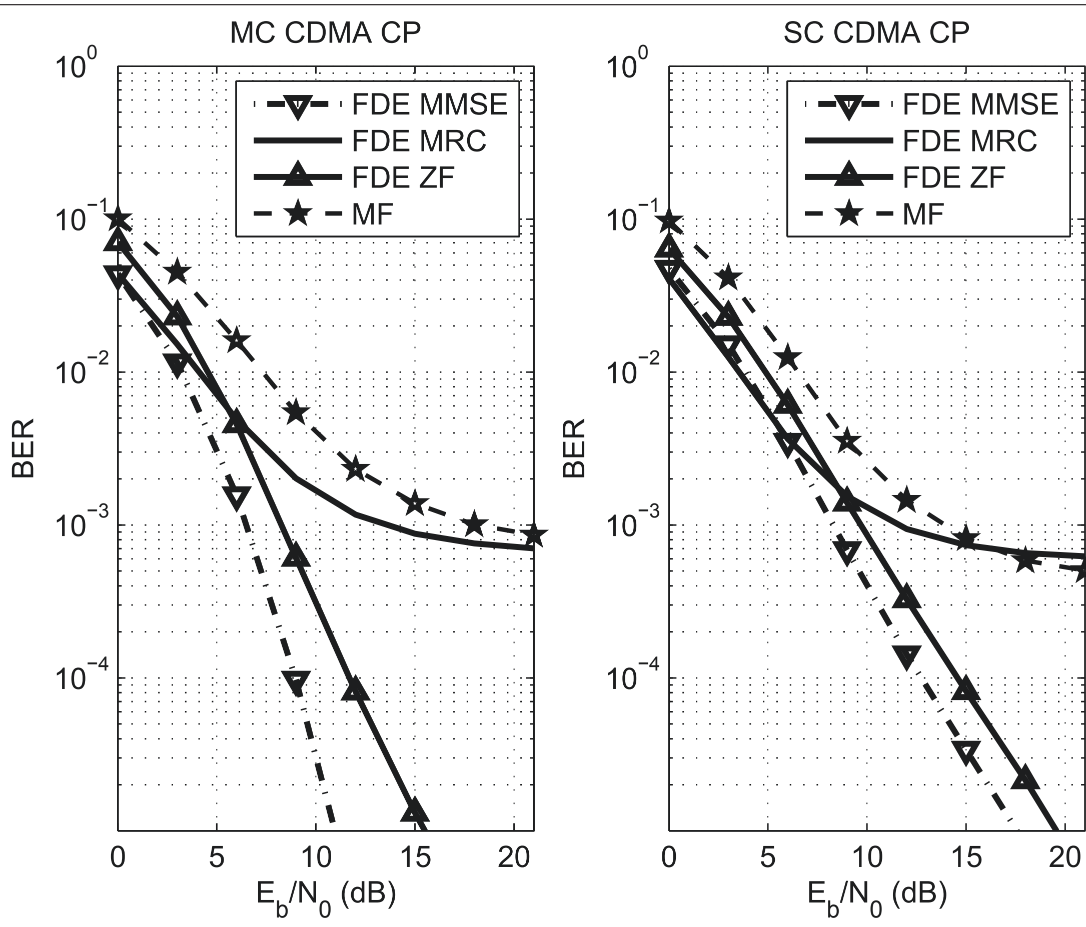

Figure 4 Performance of FDE algorithms. BER versus E_b/N_0 for CP systems.

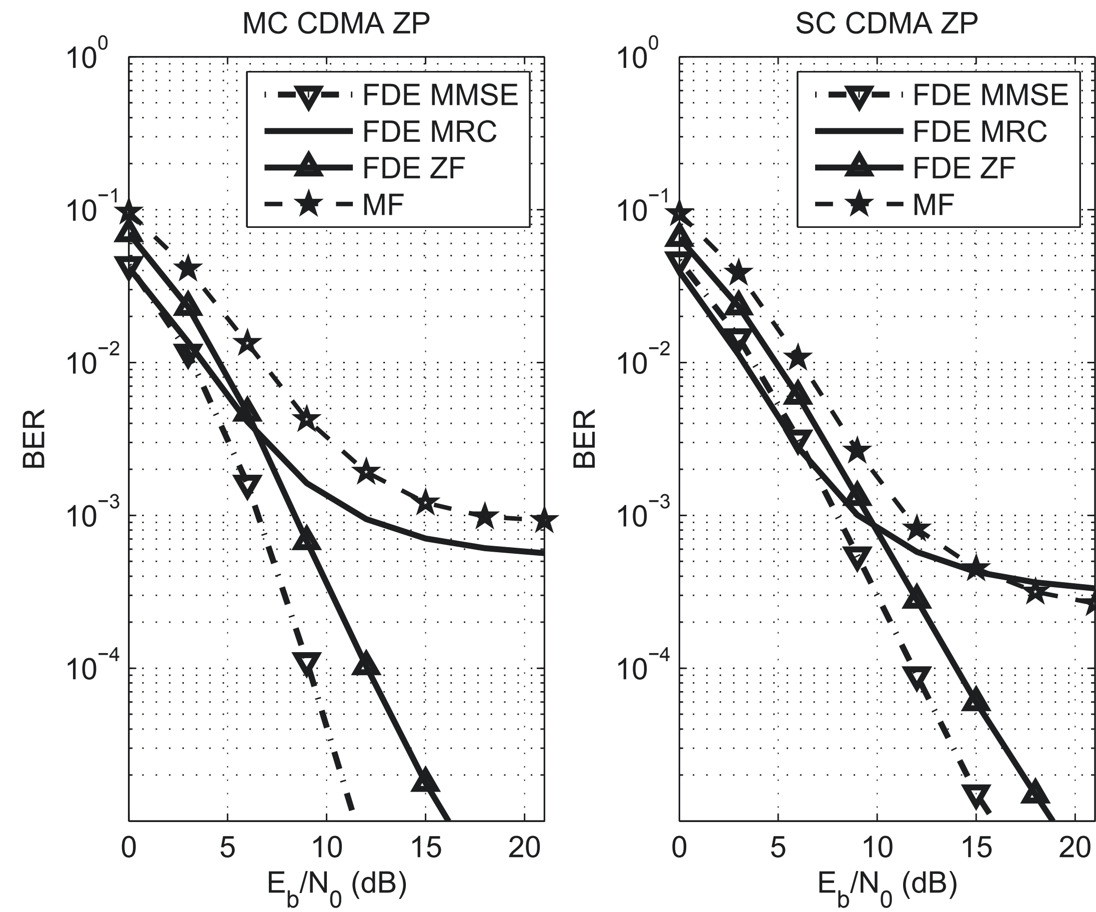

Figure 5 Performance of FDE algorithms. BER versus E_b/N_0 for ZP systems.

the first experiment. This type of channel is named Uniform in the performance curves. For the second channel we assume that the average power of each path decays exponentially, such that $|p_{j,l}|^2 = \sigma_0^2 \texttt{exp}(-l)$, l = 0, 1, 2, 3, and $\sigma_0^2 = 1 - \texttt{exp}(-1)/(1 - e^{-L})$[28]. This channel is named as Exponential in the figures. Finally, the third channel results from the multiplication of a matrix $\tilde{\boldsymbol{K}}$ by the channel vector generated as in the Exponential channel case. Matrix $\tilde{\boldsymbol{K}}$ was randomly generated and normalized such that the average power in each path is kept constant. This third channel is termed Correlated in the figures.

As in the two first experiments, we set a system with K = 4 users using Hadamard codes of length M = 16 and the guard interval length is L_{gi} = 3. FDE with zero forcing single user receiver (FDE ZF) was employed.

The BER results for CP systems are shown in Figure 6, and ZP systems results are shown in Figure 7. As expected, the receiver performs worst for Correlated channels due to smaller coding gain that the systems exhibit for this type of channels (see Appendix).

5.4 Performance for different user codes

In this experiment we assess the BER for different codes. Four types of user codes are considered: Pseudo-noise sequences (PN), Walsh-Hadamard, Vandermonde and Zadoff-Chu (ZC) codes [29,30], all of length 16. Vandermonde codes are taken from the columns of the Vandermonde matrix:

$$\boldsymbol{C} = \frac{1}{\sqrt{\varpi}} \begin{bmatrix} \varepsilon_0 & \varepsilon_0^2 & \cdots & \varepsilon_0^K \\ \varepsilon_1 & \varepsilon_1^2 & \cdots & \varepsilon_1^K \\ \vdots & \vdots & \ddots & \vdots \\ \varepsilon_{M-1} & \varepsilon_{M-1}^2 & \cdots & \varepsilon_{M-1}^K \end{bmatrix} \quad (29)$$

where $\frac{1}{\sqrt{\varpi}}$ normalizes the codes, such that $\boldsymbol{c}_k^H \boldsymbol{c}_k = 1$. The parameters ε_j can be chosen as equispaced points on the unit circle by setting $\varepsilon_j = \texttt{exp}\left(-\sqrt{-1}j(2\pi/M)\right)$, j = 0, 1, ..., M - 1 [31]. In this system $\varepsilon_j = \texttt{exp}\left(-\sqrt{-1}j(2\pi/M)\right)$, j = 0, 1, ..., M - 1.

We consider a scenario with K = 4 users and time-variant channels as in the first two experiments. In each run, the user codes were randomly chosen. BER results

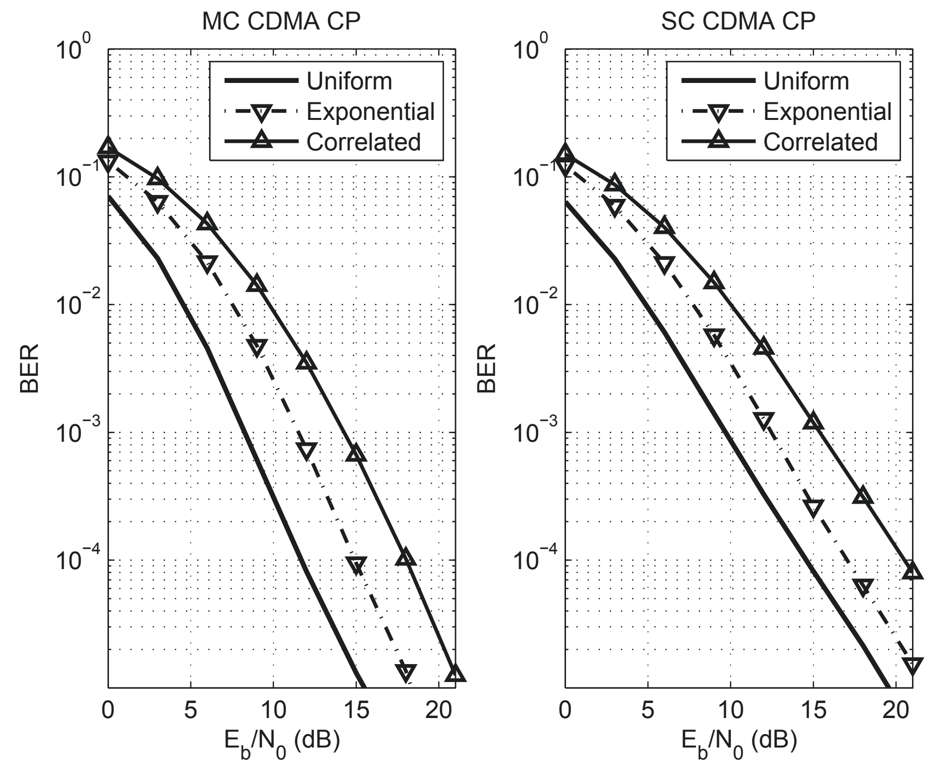

Figure 6 Performance for different type of channels. BER versus E_b/N_0 for CP systems.

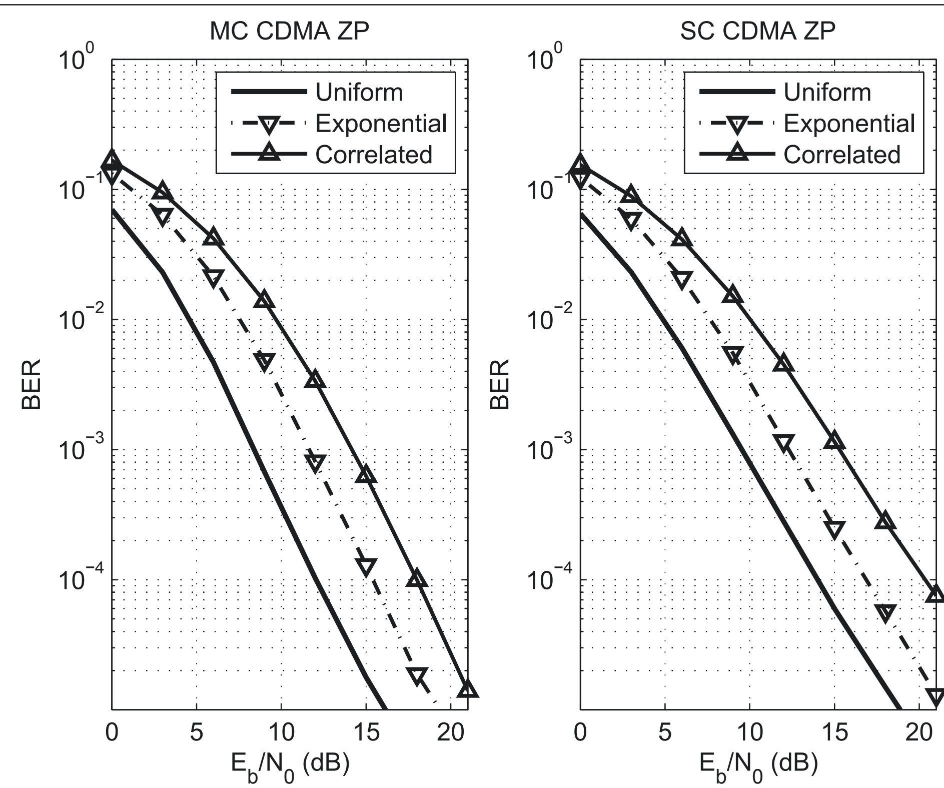

Figure 7 Performance for different type of channels. BER versus E_b/N_0 for ZP systems.

are shown in Figures 8 and 9 for the zero forcing single user FDE receiver (FDE ZF). We recall that for the multicarrier transmission system with CP as guard interval, the use of Vandermonde codes allows the maximum diversity gain when multi-user maximum likelihood detection is employed. Note, however, that the considered FDE ZF receiver (which is suboptimum) also exploits the diversity gain of the system in this case. For single carrier transmission system with CP as guard interval, it can be verified that the use of Vandermonde codes leads to a single carrier TDMA transmission system with ZP (in this case, $\boldsymbol{V} = \boldsymbol{F}_M^H \boldsymbol{C} = \boldsymbol{I}_{M\times K}$, where $\boldsymbol{I}_{M\times K}$ is a truncated identity matrix), and the results in Figure 8 indicate that the FDE was not able to exploit the diversity gain.

The FDE ZF receiver for systems using Hadamard codes does not exploit the diversity gain of the system, but presents a better coding gain, as expressed by the offset on the BER curve. On the other hand, the use ZC or PN codes yields to better exploiting the coding gain of the systems, as shown by the bigger slope of the BER curve.

6 Conclusion

This work proposed a FDE STBC CDMA-based transmission system. The FDE algorithms used with single user detection resulted in a simple receiver design with reduced computational complexity. Simulations results have shown good performance in terms of BER when compared to previously proposed STBC CDMA systems. Diversity and coding gain analysis of the proposed structure was performed and conditions to achieve their maximum values, with multiuser maximum likelihood detection, were identified.

Note

[1]See equation (29).

Appendix

Diversity and Coding Gain Analysis

Let us drop the time index and use only one equation from (15). If for a given detection system $P(\varepsilon_k|\boldsymbol{h}_0, \boldsymbol{h}_1)$ is the conditional error probability of user k, then

$$P(\varepsilon_k|\boldsymbol{h}_0,\ \boldsymbol{h}_1) \le P_B(\varepsilon|\boldsymbol{h}_0, \boldsymbol{h}_1) \quad (30)$$

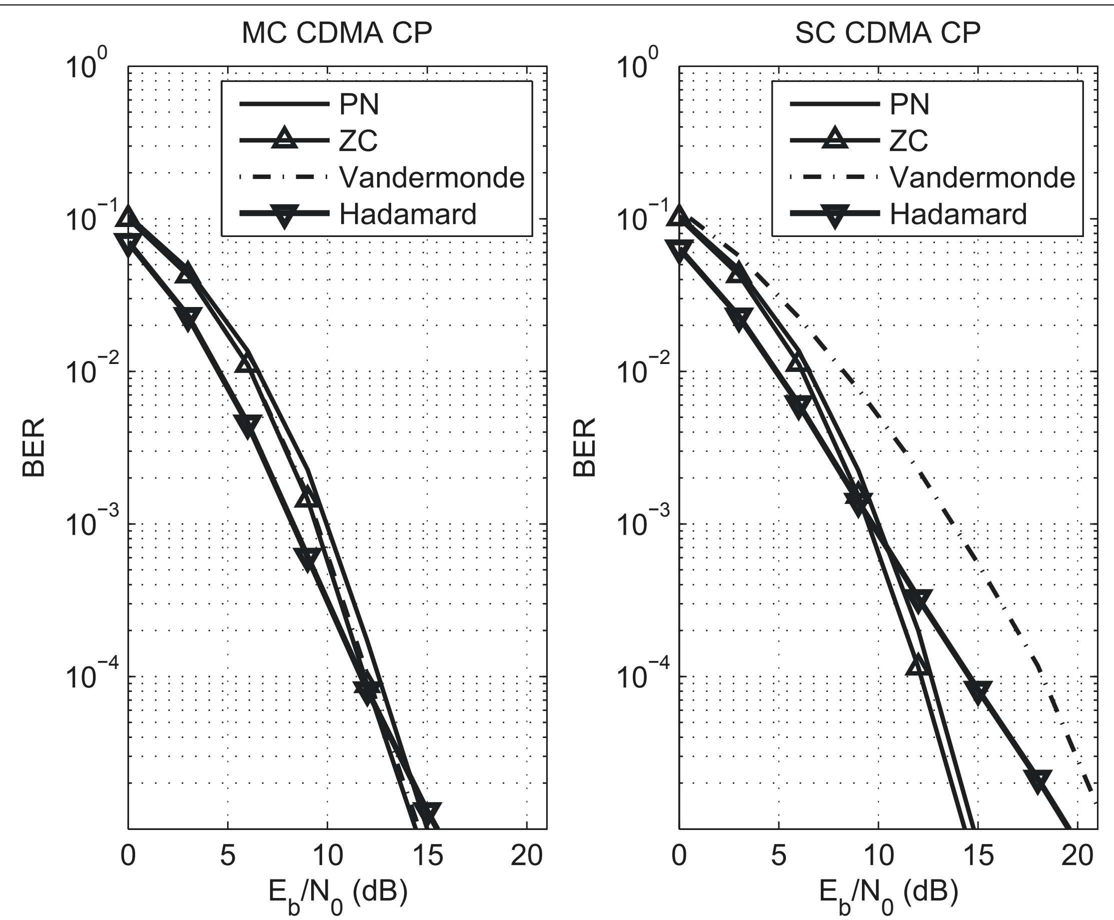

Figure 8 Performance for different type of user code. BER versus E_b/N_0 for CP systems.

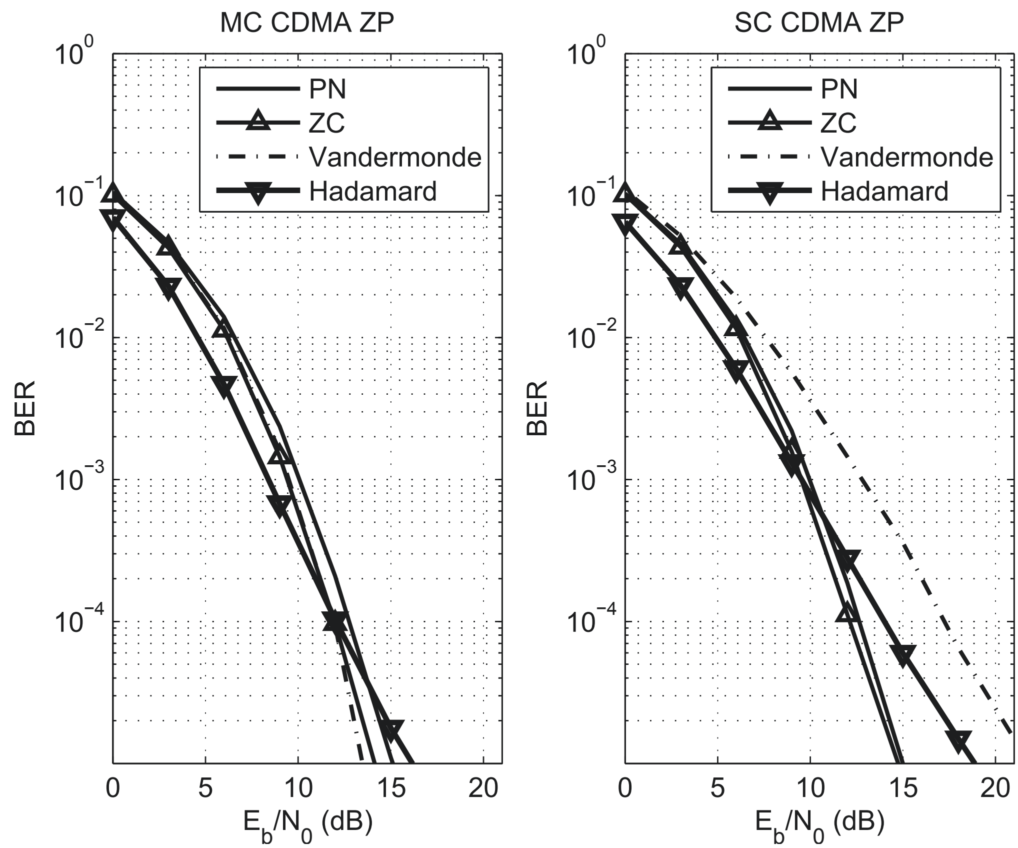

Figure 9 Performance for different type of user code. BER versus E_b/N_0 for ZP systems.

where $P_B(\cdot)$ is the block (block of symbols of K users) error probability and is given by

$$P_B(\varepsilon|\boldsymbol{h}_0,\ \boldsymbol{h}_1) = \sum_{s\in\chi}\sum_{\substack{\hat{s}\in\chi\\ \hat{s}\neq s}} P(\hat{\boldsymbol{s}}|\boldsymbol{s},\boldsymbol{h}_0,\ \boldsymbol{h}_1)P(\boldsymbol{s}|\boldsymbol{h}_0,\ \boldsymbol{h}_1) \tag{31}$$

where χ represents the set of possible values for $\boldsymbol{s}$ and $P(\hat{\boldsymbol{s}}|\boldsymbol{s},\ \boldsymbol{h}_0,\ \boldsymbol{h}_1)$ is the conditional probability of the event that the detected block is $\hat{\boldsymbol{s}}$ when the transmitted block is $\boldsymbol{s}(\hat{\boldsymbol{s}} \neq \boldsymbol{s})$.

Using standard procedures, we arrive, for equiprobable symbols at

$$P(\varepsilon_k) \leq \frac{1}{|\chi|}\sum_{e\neq 0}\vartheta(\boldsymbol{e})f(\boldsymbol{e}) \tag{32}$$

where $|\chi|$ denotes the cardinality of χ, $\boldsymbol{e} = \hat{\boldsymbol{s}} - \boldsymbol{s}$, $\vartheta(\boldsymbol{e})$ is the number of occurrences of a given vector $\boldsymbol{e}$, when $\hat{\boldsymbol{s}}$ and $\boldsymbol{s}$ span χ, $f(\boldsymbol{e}) = \mathbb{E}\,[\exp(-||\boldsymbol{\Lambda}_{01}\boldsymbol{Ve}||^2\gamma)]$ and $\gamma = \tilde{E}_s/SN_0$.

Let $\boldsymbol{K} = \mathbb{E}\left[\boldsymbol{h}_j\boldsymbol{h}_j^H\right]$ be the covariance matrix of the channel vector $\boldsymbol{h}_j(j = 0,\ 1)$, where it was assumed that the channels $\boldsymbol{h}_j$ are identically distributed. Since $\boldsymbol{K}$ is square Hermitian, it always admits spectral decomposition, i.e., $\boldsymbol{K} = \boldsymbol{\Omega}\boldsymbol{D}\Omega^H$, where $\boldsymbol{D}$ is a $L \times L$ diagonal matrix whose entries are the eigenvalues of $\boldsymbol{K}$ and $\boldsymbol{\Omega}$ is a unitary matrix whose columns are the normalized eigenvectors of $\boldsymbol{K}$.

If we assume that $\boldsymbol{K}$ is non-singular and introduce the channel vector $\tilde{\boldsymbol{h}}_j = \boldsymbol{D}^{-1/2}\boldsymbol{\Omega}^H\boldsymbol{h}_j$, which by construction has a identity covariance matrix, then we can write

$$||\boldsymbol{\Lambda}_{01}\boldsymbol{V}\ \boldsymbol{e}||^2\ = \sum_{j=0}^{1}\tilde{\boldsymbol{h}}_j^H\boldsymbol{\Gamma}(\boldsymbol{e})\tilde{\boldsymbol{h}}_j. \tag{33}$$

where

$$\boldsymbol{\Gamma}(\boldsymbol{e}) = [\boldsymbol{D}^{1/2}]^H\boldsymbol{\Omega}^H\boldsymbol{\Gamma}_0(\boldsymbol{e})\boldsymbol{\Omega}\boldsymbol{D}^{1/2} \tag{34}$$

$$\boldsymbol{\Gamma}_0(\boldsymbol{e}) = \tilde{\boldsymbol{F}}_{Q\times L}^H\text{diag}^H(\boldsymbol{V}\ \boldsymbol{e})\text{diag}(\boldsymbol{V}\ \boldsymbol{e})\tilde{\boldsymbol{F}}_{Q\times L}. \tag{35}$$

If the channels $\boldsymbol{h}_0$ and $\boldsymbol{h}_1$ are modeled as statistically independent complex gaussian vectors, then after some algebraic manipulation, we obtain for $f(\boldsymbol{e})$ in (32):

$$f(\boldsymbol{e}) = \prod_{l=0}^{\kappa(\boldsymbol{e})-1}\left(\frac{1}{(1+\gamma\lambda_l(\boldsymbol{e}))}\right)^2 \tag{36}$$

$$\leq \frac{1}{\left(\gamma^{\kappa(e)} \prod_{l=0}^{\kappa(e)-1} \lambda_l(e)\right)^2} \tag{37}$$

where $\lambda_l(\boldsymbol{e})$ are the eigenvalues of $\boldsymbol{\Gamma}(\boldsymbol{e})$ and $\kappa(\boldsymbol{e})$ is the rank of $\boldsymbol{\Gamma}(\boldsymbol{e})$. Substituting (37) into (32) we arrive at

$$P(\varepsilon_k) \leq \frac{1}{|\chi|} \sum_{e \neq 0} \frac{\vartheta(e)}{\left(\gamma \left[\prod_{l=0}^{\kappa(e)-1} \lambda_l(e)\right]^{\frac{1}{\kappa(e)}}\right)^{2\kappa(e)}}. \tag{38}$$

From (34) we have that if $\boldsymbol{K}$ is full rank, then $\kappa(\boldsymbol{e}) = \mathtt{rank}(\boldsymbol{\Gamma}(\boldsymbol{e})) = \mathtt{rank}(\boldsymbol{\Gamma}_0(\boldsymbol{e}))$, and its maximum value is L ($\boldsymbol{\Gamma}_0(\boldsymbol{e})$ is an $L \times L$ matrix). The system is said to achieve maximum diversity gain if $\min_{\boldsymbol{e} \neq \boldsymbol{0}} \kappa(\boldsymbol{e}) = L$, and thus, $\kappa(\boldsymbol{e}) = L$, $\forall \boldsymbol{e} \neq \boldsymbol{0}$. That is, $\boldsymbol{\Gamma}(\boldsymbol{e})$ is a full rank matrix for any $\boldsymbol{e} \neq \boldsymbol{0}$. We note from (33) that this is equivalent to have $||\boldsymbol{\Lambda}_{01} \boldsymbol{V} \boldsymbol{e}||^2 \neq \boldsymbol{0}$ for any vector $\boldsymbol{e} \neq \boldsymbol{0}$. Under this condition we have

$$\begin{aligned} P(\varepsilon_k) &\leq \frac{1}{|\chi|} \sum_{e \neq 0} \frac{\vartheta(e)}{\left(\gamma \left[\prod_{l=0}^{L-1} \lambda_l(e)\right]^{\frac{1}{L}}\right)^{2L}} \\ &= \frac{1}{|\chi|} \sum_{e \neq 0} \frac{\vartheta(e)}{\left(\gamma [\det(\boldsymbol{\Gamma}(e))]^{\frac{1}{L}}\right)^{2L}}, \end{aligned} \tag{39}$$

where $\mathtt{det}(\cdot)$ denotes determinant.

We remark that since the diversity gain depends only on $\boldsymbol{\Gamma}_0(\boldsymbol{e})$ given by (35), it does not depend on the channel covariance matrix $\boldsymbol{K}$ (provided that is non-singular). It depends, however, on the particular system employed and the relative power of the users.

From (34) we have that if $\boldsymbol{K}$ is full rank,

$$\begin{aligned} \det(\boldsymbol{\Gamma}(e)) &= \det([\boldsymbol{D}^{1/2}]^H \boldsymbol{\Omega}^H \boldsymbol{\Omega} \boldsymbol{D}^{1/2}) \det(\boldsymbol{\Gamma}_0(e)) \\ &= \det(\boldsymbol{D}) \det(\boldsymbol{\Gamma}_0(e)) = \det(\boldsymbol{K}) \det(\boldsymbol{\Gamma}_0(e)). \end{aligned}$$

It then results from (39) that for a system that attains maximum diversity gain:

$$\begin{aligned} P(\varepsilon_k) &\leq \frac{1}{|\chi|} \sum_{e \neq 0} \frac{\vartheta(e)}{\left(\gamma [\det(\boldsymbol{K}) \det(\boldsymbol{\Gamma}_0(e))]^{\frac{1}{L}}\right)^{2L}} \\ &\leq \frac{1}{\left(\gamma [\det(\boldsymbol{K}) \min_{e \neq 0} \det(\boldsymbol{\Gamma}_0(e))]^{\frac{1}{L}}\right)^{2L}} \frac{1}{|\chi|} \sum_{e \neq 0} \vartheta(e) \\ &= \frac{1}{[\gamma G_c]^{2L}} (|\chi| - 1), \end{aligned}$$

with $G_c = g_0[\mathtt{det}(\boldsymbol{K})]^{1/L}$, where $g_0 = [\min_{\boldsymbol{e} \neq \boldsymbol{0}} \mathtt{det}(\boldsymbol{\Gamma}_0(\boldsymbol{e}))]^{1/L}$, being the coding gain. As the trace of $\boldsymbol{K} = \mathtt{E}[||\boldsymbol{h}||^2] = 1$ then $\mathtt{det}(\boldsymbol{K}) < 1$ and the maximum value of $\mathtt{det}(\boldsymbol{K})$ is obtained when all the eigenvalues of $\boldsymbol{K}$ are the same, i.e., $\lambda_{\boldsymbol{K},i} = 1/L$ ($i = 1, 2, \ldots, L$). In this case $\mathtt{det}(\boldsymbol{K}) = (1/L)^L$, and therefore, for a system transmitting in a channel with L multipath components

$$G_c \leq g_0 \left(\frac{1}{L}\right) \tag{40}$$

equality (maximum coding gain) is achieved, for example, when channel has uncorrelated equal power coefficients ($\boldsymbol{K} = L^{-1}\boldsymbol{I}$).

Abbreviations

BER: bit error rate; CIBS: chip-interleaved block-spread; CP: cyclic prefix; DS-CDMA: direct-sequence code division multiple access; FDE: frequency domain equalization; FIR: finite-impulse response; IBI: interblock interference; ISI: intersymbol interference; MMSE: minimum mean squared error; MRC: maximal ratio combiner; OFDM: orthogonal frequency division multiplexing; RLS: recursive least squares; SC-FDE: single-carrier frequency-domain equalization; STBC: space-time block-coded; ZP: zero padding.

Acknowledgements

This study was supported by the Brazilian Council for Scientific and Technological Development (CNPq).

Competing interests

The authors declare that they have no competing interests.

Received: 1 December 2010 Accepted: 30 August 2011
Published: 30 August 2011

References

1. S Alamouti, A simple transmit diversity technique for wireless communications. IEEE J Sel Areas Commun. **16**(8), 1451–1458 (1998). doi:10.1109/49.730453
2. V Tarokh, H Jafarkhani, AR Calderbank, Space-time block codes from orthogonal designs. IEEE Trans Inf Theory **45**(5), 1456–1467 (1999). doi:10.1109/18.771146
3. V Tarokh, N Seshadri, AR Calderbank, Space-time codes for high data rate wireless communication: performance criterion and code construction. IEEE Trans Inf Theory **44**(2), 744–765 (1998). doi:10.1109/18.661517
4. B Hochwald, TL Marzetta, CB Papadias, A transmitter diversity scheme for wideband CDMA systems based on space–time spreading. IEEE J Sel Areas Commun. **19**, 1 (2001). doi:10.1109/JSAC.2001.909604
5. H Li, X Lu, GB Giannakis, Capon multiuser receiver for CDMA systems with space–time coding. IEEE Trans Signal Process. **50**(5), 1193–1204 (2002). doi:10.1109/78.995086
6. Z Liu, GB Giannakis, S Barbarossa, A Scaglione, Transmit antennae space–time block coding for general OFDM in the presence of unknown multipath. IEEE J Sel Areas Commun. **19**(7), 1352–1364 (2001). doi:10.1109/49.932702
7. E Lindsok, A Paulraj, A transmit diversity scheme for delay spread channels, in *Proceedings of the IEEE International Conference on Communications*, New Orleans, USA, 307–311 (2000)
8. FW Vook, TA Thomas, Transmit diversity schemes for broadband mobile communication systems, in *Proceedings of the IEEE Vehicular Technology Conference Fall (VTC2000)*. **6**, 2523–2529 (2000)
9. N Al-Dhahir, Single-carrier frequency-domain equalization for space–time block-coded transmission over frequency-selective fading channels. IEEE Commun Lett. **5**(7), 304–306 (2001). doi:10.1109/4234.935750
10. F Pancaldi, GM Vitetta, R Kalbasi, N Al-Dhahir, M Uysal, H Mheidat, Single-carrier frequency domain equalization. IEEE Signal Process Mag. **25**(5), 37–56 (2008)
11. L Song, R de Lamare, AG Burr, Successive interference cancellation schemes for time-reversal space–time block codes. IEEE Trans Veh Technol. **57**(1), 642–648 (2008)
12. RC de Lamare, M Haardt, R Sampaio Neto, Low-complexity blind adaptive MIMO receivers for CDMA systems with space–time block-codes in

multipath channels. in *Proceedings of the IEEE International Symposium on Wireless Communication Systems (ISWCS'07)*, Trondheim, 686–690 (December 2007)
13. RC de Lamare, R Sampaio-Neto, Blind adaptive MIMO receivers for space–time block-coded DS-CDMA systems in multipath channels using the constant modulus criterion. IEEE Trans Commun. **58**(1), 21–27 (2010)
14. RC de Lamare, R Sampaio Neto, Space-time adaptive reduced-rank processor for interference mitigation in DS-CDMA systems. IET Commun. **57**(2), 388–397 (2008)
15. R de Lamare, A Hjorungnes, R Sampaio Neto, Adaptive MIMO decision feedback reduced rank equalization based on joint iterative optimization of adaptive RLS estimation algorithms, in *Proceedings of the IEEE Wireless Communications and Networking Conference*, Las Vegas, USA, 413–418 (April 2008)
16. CA Medina, TTV Vinhoza, R Sampaio-Neto, A blind channel estimation algorithm for space–time coded MC-CDMA receivers. in *Proceedings of the IEEE International Conference on Communications*, Dresden (June 2009)
17. S Zhou, GB Giannakis, C Le Martret, Chip-interleaved block-spread code division multiple access. IEEE Trans Commun. **50**, 235–248 (2002). doi:10.1109/26.983320
18. F Petre, G Leus, L Deneire, M Engels, M Moonen, H De Man, Space-time block coding for single-carrier block transmission DS-CDMA downlink. IEEE J Sel Areas Commun. **21**(3), 350–361 (2003). doi:10.1109/JSAC.2003.809630
19. Y Yang, YH Chew, TT Tjhung, Adaptive frequency-domain equalization for space–time block-coded DS-CDMA downlink, in *Proceedings of the IEEE International Conference on Communications (ICC, 2005)* **4**, 2343–2347 (2005)
20. FW Vook, TA Thomas, KL Baum, Cyclic-prefix cdma with antenna diversity, in *Proceedings of the IEEE Vehicular Technology Conference Spring (VTC2002)* **2**, 1002–1006 (2002)
21. S Zhou, G Giannakis, Single-carrier space–time block-coded transmission over frequency-selective fading channels. IEEE Trans Inf Theory **49**(1), 164–179 (2003). doi:10.1109/TIT.2002.806158
22. S Zhou, G Giannakis, Space-time coding with maximum diversity gains over frequency-selective fading channels. IEEE Signal Process Lett. **48**(10), 269–272 (2001)
23. Z Wang, GB Giannakis, Wireless multicarrier communications: where Fourier meets Shannon. IEEE Signal Process Mag. **17**(3), 29–47 (2000). doi:10.1109/79.841722
24. S Haykin, Adaptive Filter Theory (Prentice Hall, 2001)
25. PS Chang, AN Willson, Analysis of conjugated gradient algorithms for adaptive filtering. IEEE Trans Signal Process. **48**(2), 409–418 (2000). doi:10.1109/78.823968
26. K Fazel, S Kaiser, Multi-Carrier and Spread Spectrum Systems (Wiley, 2003)
27. TS Rappaport, Wireless Communications: Principles and Practice (Prentice Hall PTR, 1996)
28. T Kaitz, Channel and interference model for 802.16b physical layer, IEEE 802.16 Broadband Wireless Access Working Group. (2001)
29. RL Frank, SA Zadoff, Phase shift pulse codes with good periodic correlation properties. IEEE Trans Inf Theory **IT-8**, 381–382 (1962)
30. D Chu, Polyphase codes with good periodic correlation properties. IEEE Trans Inf Theory **18**(4), 531–532 (1972). doi:10.1109/TIT.1972.1054840
31. AS Cacciapuoti, G Gelli, F Verde, FIR zero-forcing multiuser detection and code designs for downlink MC-CDMA. IEEE Trans Signal Process. **55**(10), 4737–4751 (2007)

doi:10.1186/1687-1499-2011-80
Cite this article as: Medina and Sampaio-Neto: **Frequency domain equalization space-time block-coded CDMA transmission system.** *EURASIP Journal on Wireless Communications and Networking* 2011 **2011**:80.